Development of a Novel Test Rig to Investigate Explosion Safety in Gas Turbine Enclosures

Jan Kowalski, Martin Lauer, David Engelmann, Michele Cagna, Ronald Mailach, Francesca Di Mare

Development of a Novel Test Rig to Investigate Explosion Safety in Gas Turbine Enclosures

Jan Kowalski[1]*, Martin Lauer[2], David Engelmann[1], Michele Cagna[3], Ronald Mailach[2], Francesca di Mare[1]

ISROMAC 2017

International Symposium on Transport Phenomena and Dynamics of Rotating Machinery

Maui, Hawaii

December 16-21, 2017

Abstract

To investigate explosion safety in gas turbine enclosures, development work was conducted to design a scaled test rig of a modern MAN MGT-6100 gas turbine package. Since the focus of research is on the ventilation flow, the turbine components were designed as inactive and mainly function as flow obstructions. Analytical as well as CFD investigations were carried out to determine the model scale and to evaluate operation condition restrictions. As a result the test rig was downscaled to 1:3 and the ventilation system was chosen to accomplish different operation conditions up to Re-similarity. The design, which was optimized for PIV measurements, as well as the experimental setup will be described in detail in this paper. During development the design of the actual package was optimized further, leading to differences in component arrangement. An additional CFD model was created to consider these changes not only in the test rig. This model was subjected to a grid sensitivity analysis, and used to identify additional measurement planes for PIV investigations.

Keywords

Test Rig Development — Gas Turbine — Enclosure Ventilation — Explosion Safety

[1] *Chair of Thermal Turbomachinery, Ruhr-Universität Bochum, Bochum, Germany*

[2] *Chair of Turbomachinery and Flight Propulsion, Technische Universität Dresden, Dresden, Germany*

[3] *MAN Diesel & Turbo SE, Oberhausen, Germany*

*__Corresponding author__: jan.kowalski@rub.de

INTRODUCTION

Due to the still growing demand for more flexible power plant solutions, industry-type gas turbines of intermediate power class (up to 25 MW) have moved into the focus of research efforts over the past years, e.g. here [1]. Since the dimensions of these machines often allow being set up on a single frame they are usually designed as so-called gas turbine packages which include the electric generator on the same frame in case of a power generation setup. This specific design is commonly accompanied by the whole machine being engulfed in an acoustic enclosure. These so-called compartments reduce the emitted noise level of the gas turbine and protect it from environmental influences when operated as an outdoor installation. The enclosure separates the gas turbine from the surroundings, therefore the whole compartment has to be actively ventilated for two main reasons: Firstly, the ventilation flow removes heat losses generated from the Brayton cycle itself and thus keeps machine components at acceptable temperature levels. Secondly, the ventilation flow has to dilute and remove clouds of fuel from the compartment in case of gas leakage due to e.g. seal failure in the fuel system. Though the latter case is unlikely during engine operation it must still be considered. The British Health and Safety Executive (HSE) [2] reported 134 gas leakages in the UK over a period of 13 years leading to a total of 19 incidents of fuel ignitions in gas turbine enclosures, thus underlining the importance of careful ventilation flow design to ensure explosion safety.

To investigate in detail the mixing of a fuel leakage jet within a state-of-the-art MGT-6100 gas turbine package from MAN Diesel & Turbo SE, Petrick [3] conducted CFD investigations using ANSYS CFX with the k-ω SST turbulence model on the whole compartment, taking into account thermal convection as well as leakages at different positions. Petrick concluded that the current package design meets modern explosion safety requirements but underlines the importance of applying appropriate boundary conditions for heat transfer. Therefore, a research project was launched aimed at creating validation data for CFD investigations in a test rig of the aforementioned gas turbine package, which will be discussed in this paper. The focus, however, will be on the design process and numerical results.

1. PROJECT GOALS AND APPROACH

Development work was carried out with three distinct long-term goals to accomplish: Firstly, validation data for CFD investigations shall be created for cold, heated, as well as leakage configuration. Secondly, a detailed experimental and numerical assessment of heat transfer and buoyancy effects shall be conducted in different operation conditions including cases of fan failure. Lastly, the optimization potential of reducing or redirecting the ventilation flow will be explored.

To fulfill the defined goals a scaled test rig of the gas turbine enclosure was designed, which can be seen in figure 1. The test rig features all relevant components of the machine, including the gas turbine, gear, generator, as well as complex pipework of the oil and fuel system in reasonably simplified

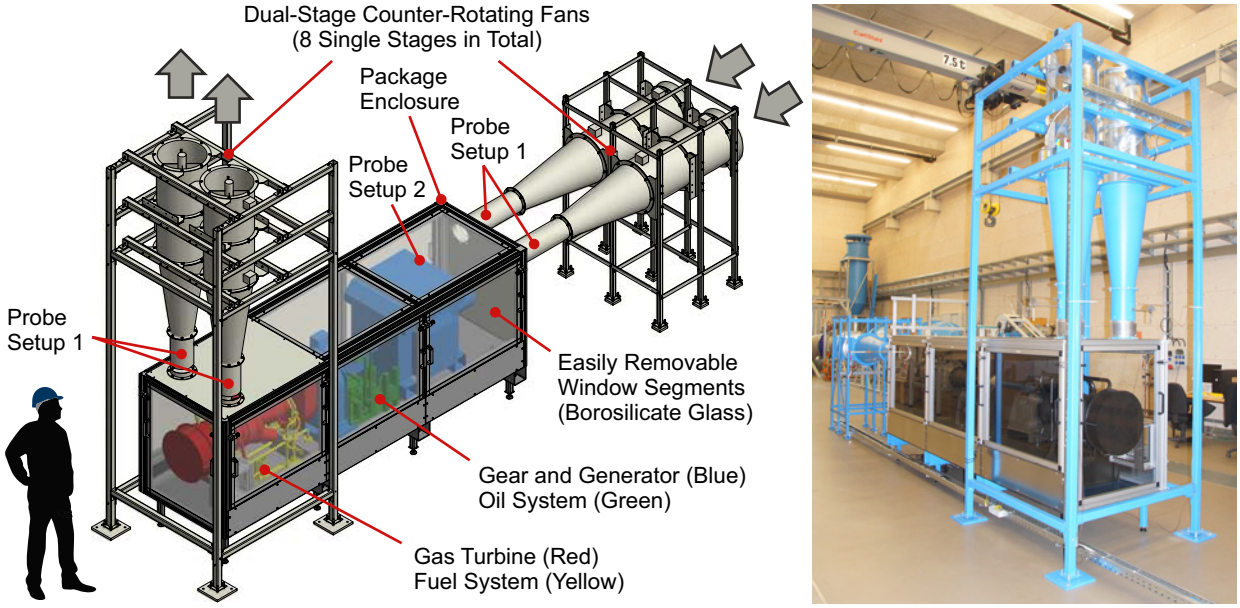

(a) CAD model

(b) Assembled test rig

Figure 1. Final construction of the downscaled (1:3) package test rig

degree of detail. The machine itself is inactive and mainly functions as an obstacle for the ventilation flow. Initially the test rig will be set up in cold configuration but the later addition of heating elements and gas leakage (CO_2 model gas) is considered. The following design process and corresponding numerical studies were carried out at the Ruhr-Universität Bochum in cooperation with the Technische Universität Dresden where the test rig will be investigated experimentally at the Centre for Energy Technology.

2. TEST RIG DESIGN PROCESS

The focus of the design process was on creating an easily accessible and modifiable test rig at reasonable cost and construction effort while pushing the limits of complexity seen in related experimental investigations in the open literature, i.e. from Vahidi *et al.* [4].

2.1 Description of the Flow Phenomena

Prior to designing the test rig geometry, relevant aspects of the regarded flow field were identified and taken into account in terms of similarity and transferability of the scaled results to the real-size machine. Therefore, the flow inside the regarded containment was broken down into four main flow phenomena, namely:

a) Separated flow around bluff bodies
b) Interaction of the internal generator cooling flow (IGCF) with the main enclosure ventilation flow (MEVF) during extraction and reentry into the enclosure
c) Thermal buoyancy near the hot engine surfaces
d) Interaction of occurring fuel leakage jets with the MEVF (in case of e.g. seal failure)

While flow separation zones can be observed within the whole compartment, the other phenomena are restricted to specific areas of the enclosure as briefly illustrated in figure 2.

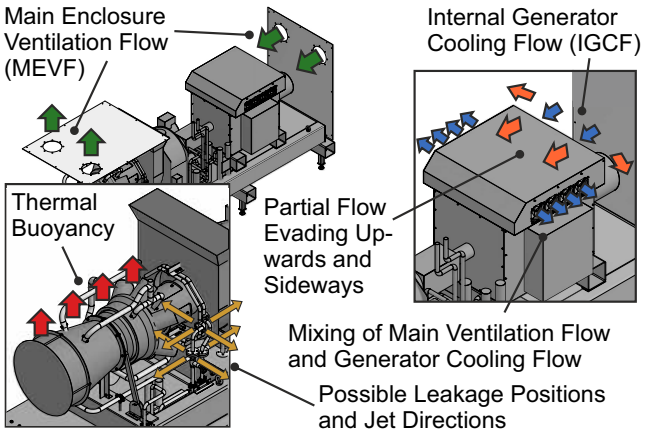

Figure 2. Overview of the flow phenomena inside the enclosure

The regarded gas turbine system features an electric power generator on the base frame which is actively ventilated, leading to the aforementioned interaction of the IGCF with the MEVF at the generator in- and outlets. In the actual engine the primary air supply for the Brayton cycle process and the resulting exhaust flow are guided through separate assemblies and do not interact with the MEVF, apart from heat transfer effects: Waste heat from the process is transferred to the ventilation air overflowing the hot gas turbine components, leading to changes in fluid density and therefore causing buoyancy convection effects. Unlike the first three flow aspects, which occur during regular engine operation,

fuel leakage is regarded as a case of system failure, which has to be considered, as already mentioned. Fuel leakage would most likely be caused by a seal or welding seam failure within the fuel system. In such cases the fuel gas release can be assumed to occur as a choked fuel jet interacting with the MEVF, according to Ivings *et al.* [5].

Apparently the flow inside the compartment is highly complex and especially the separation flow interacts significantly with the other flow phenomena. Since not all similarity quantities can be matched during testing, an analytical and CFD-based design study was carried out to identify a suitable model scale and to derive requirements for the test rig and ventilation system design.

2.2 Analytical Design Study

Vahidi *et al.* [4] conducted similar research on a scaled gas turbine package with greatly simplified geometry featuring heated gas turbine surfaces as well as leakage with carbon dioxide (CO_2) as model gas. They concluded that for hydraulic and thermal analogy a scaled test rig has to be operated with the same Reynolds (Re), Nusselt (Nu) and Grashof (Gr) number as the actual engine [4]. They are calculated as given in equations 1 - 3 with c being the velocity at the package inlets, D the inlet duct diameter, ν the kinematic viscosity, h the heat transfer coefficient, L the characteristic length, k the fluid's thermal conductivity, g the gravitational acceleration, β the fluid's coefficient of thermal expansion, and ΔT the difference between the average temperature of the hot gas turbine walls and the ambient temperature T. This given set of similarity quantities allows statements on heat transfer, natural convection as well as general flow structures. However, the ratio of buoyancy and ventilation flow inertia is yet left unregarded. For model testing of flue gas extraction systems in civil engineering the Archimedes (Ar) number is commonly regarded for that purpose according to the Verein Deutscher Ingenieure e.V. (VDI) [6], as given in equation 4. The VDI furthermore recommends test rigs incorporating buoyancy effects to be set up as big as possible with scaling factors k smaller than 20 and a height of the ventilated volume greater than 300 mm [6].

$$Re = \frac{cD}{\nu} \quad (1) \qquad Nu = \frac{h\,L}{k} \quad (2)$$

$$Gr = \frac{g\,\beta\,\Delta T\,L^{3}}{\nu^{2}} \quad (3) \qquad Ar = \frac{g\,\Delta T\,L}{T\,c^{2}} \quad (4)$$

Due to safety regulations at the test facility the maximum permissible wall temperature of the heated gas turbine components was limited to 230 °C, which is close to the 232 - 249 °C boiling temperature of the DEHS seeding particles used for PIV measurements. With a given limit for the wall temperature only the scaling factor k and the enclosure inlet velocity c remain as free design parameters. For a specific value of k the inlet velocity is given depending on the similarity quantity to satisfy during testing, therefore only one quantity can be matched exactly during testing.

For assessment of the degree of deviation for certain flow variables or dimensionless quantities ϕ, the ratio factor f_ϕ is introduced and defined as given in equation 5, where the subscript M indicates the corresponding value for the scaled test rig model and the subscript O the value for the real-size machine.

$$f_\phi = \frac{\phi_M}{\phi_O} \quad (5)$$

Deviations in operation conditions between the real-scale machine and the test rig configuration, i.e. the influence of different fluid inlet temperature and pressure on fluid properties, were considered during the design process for determining the correct volume flow rates for Ma- and Re-similarity (see table 2). However, fluid properties and operation conditions are regarded as identical for both configurations during the following analysis:

$$f_{Pr} = f_g = f_\nu = f_T = 1 \quad (6)$$

To evaluate f_{Nu} a simplification approach is taken by approximating the heat transfer process around the hot gas turbine components with the heat transfer characteristic of a hot cylinder being cooled by a uniform flow under an angle of 40° to the cylinder axis. The cylinder dimensions were chosen to fit the length and surface area of the hot engine components. For the assessment of Nu free and forced convection with laminar and turbulent proportions have been taken into account, as specified in the VDI Heat Atlas [7].

The results of the analytical design study are displayed in figure 3 showing f_{Ar}, f_{Gr} and f_{Nu} for different model scales and operation conditions. The different symbols hereby identify the operation conditions named after the similarity quantity, which was set up by changing the inlet duct velocity of the enclosure ventilation flow. The suffix T232 indicates an operation condition in which the maximum wall temperature is reduced to 232 °C due to staff safety concerns, i.e. OP-Re would indicate an operation point, where Re-similarity is set up at the inlet duct with real-scale wall temperatures.

When the test rig is operated in Ma-similarity condition Ar is decreased with deviations remaining within one order of magnitude for all regarded model scales, even under reduced wall temperatures, as seen in figure 3*a*. For Re-similarity the deviation of Ar increases, leading to discrepancies greater than one order of magnitude for scaling factors greater than two in both wall temperature configurations. Since Gr only accounts for the natural convection aspect of the flow, figure 3*b* shows no dependency of the inlet velocity. Similar to f_{Ar} in OP-Re and OP-Re T232 it deviates for more than one order of magnitude for scaling factors greater than two in both wall temperature configurations. Although the results indicate choosing $k = 2$ for the test rig, this model scale was regarded as unfeasible for PIV measurements due to the resulting large construction height and measurement planes as well as for the high consumption of seeding particles needed during open cycle operation. Finally, $k = 3$ was

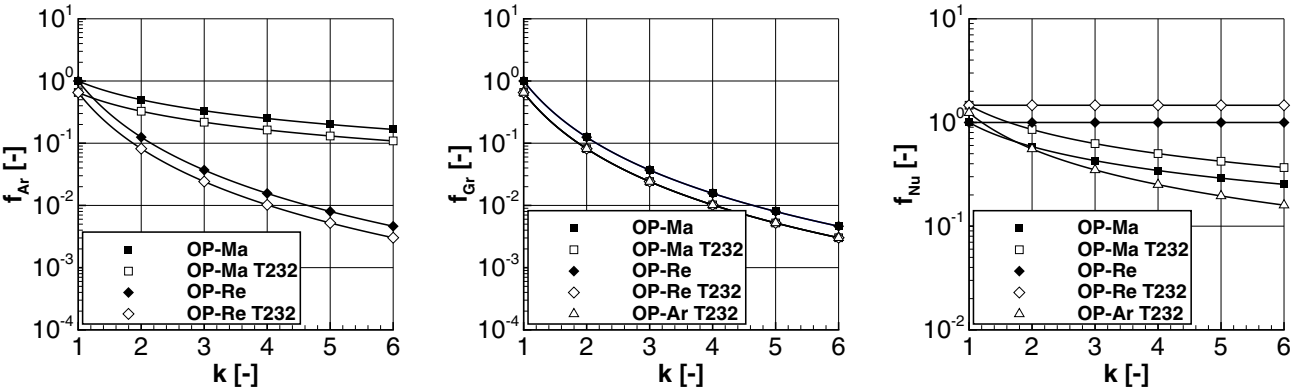

(a) Ar **(b)** Gr **(c)** Nu

Figure 3. Influence of model scale factor and test rig operation condition on selected similarity quantities

chosen for the test rig to prevent Ar and Gr from deviating two orders of magnitude ($k = 4$) compared to the real-scale machine.

Regarding f_{Nu} as illustrated in figure 3c, both Ar- and Ma-similarity operation condition lead to decreased heat transfer characteristics of the test rig, as expected. For OP-Re T232 f_{Nu} is increased compared to OP-Re with higher wall temperatures because the heat transfer is dependent on the local Re number around the gas turbine with fluid properties at mean temperature levels. As already stated OP-Re only indicates Re-similarity at the package inlet. By decreasing the wall temperature the mean density of the fluid near the gas turbine increases, which in term results in better cooling capabilities in relation to the given temperature gradient and therefore a higher Nu number. Although deviations of Gr appear to be rather large, they have little influence on the heat transfer for OP-Re and OP-Re T232, since f_{Nu} is almost independent of k (figure 3c). This indicates that forced convection is dominating the heat transfer characteristic inside the enclosure. However, the calculation of Nu was carried out under several simplifications, e.g. uniform overflow of the gas turbine components. Since the real flow field also features stagnation zones, in which natural convection can play a dominant role, Gr as well as Ar have to be considered nonetheless. To achieve Nu-similarity while operating with reduced wall temperatures, the inlet velocity can be reduced to $Re_{OP-Nu} = 0.735 \cdot Re_{OP-Re\ T232}$ while for investigations on stagnation regions and leakages operating the test rig in Ma-similarity condition is recommended, as will be outlined in the following CFD study.

2.3 CFD Design Study

Due to the complexity of the flow phenomena, assumptions and simplifications had to be made, especially for the assessment of Nu, in order to carry out the analytical study. To account for the interaction of the different flow effects, the design process was accompanied by CFD investigations based on the work of Petrick [3] using ANSYS CFX 17.0. The numerical grid used by Petrick was chosen based on an intensive grid resolution and grid type study comparing hexahedrons, tetrahedrons, and tetrahedrons combined with prism elements. The chosen mesh consists of about 15.5 million tetrahedron elements including prism layers near bounding walls. This numerical model was modified and used as the design study model (DSM), with the surface mesh shown in figure 4 and the numerical setup given in figure 5 and in table 1.

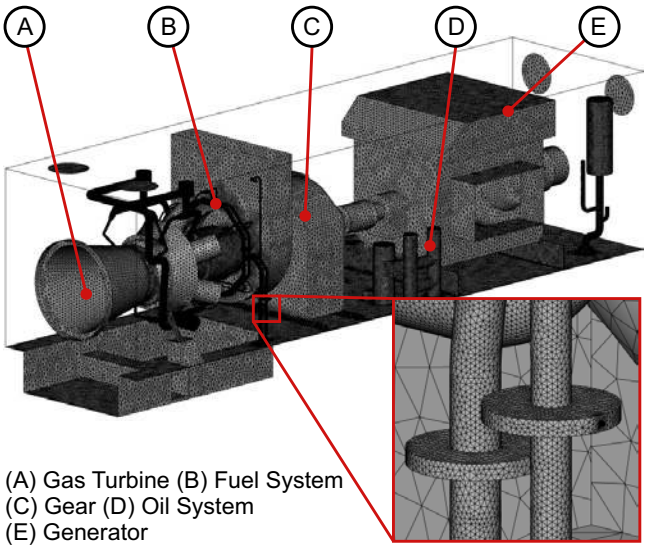

Figure 4. Surface Mesh of the numerical base model [3] modified and used as the design study model (DSM)

As already mentioned, the CFD model features all relevant flow phenomena of the enclosure flow outlined beforehand in section 2.1. During the numerical design study a CFD model with the chosen scaling factor $k = 3$ was derived from the existing one, investigated in detail, and compared to the real-scale results using CFD methods. The simulations were carried out in Ma- and Re-similarity operation condition achieved by varying the volume flow rate entering the package and the flow passing through the actively

ventilated generator respectively (boundary condition 3, 4 and 5 in figure 5). Investigations on the influence of the IGCF were conducted, such as varying the exit angle as well as leaving the generator cooling flow (3,4) out of the CFD model completely. The results underline the influence of the IGCF on the overall pressure loss as well as on heat transfer effects (waste heat removed from the generator electrics), thus the generator cooling flow (3,4) was chosen to be included in the test rig assembly.

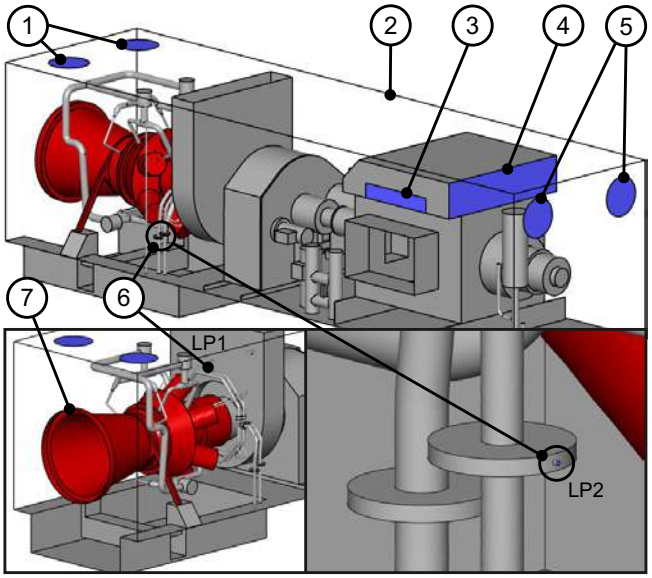

(1) Package Outlet (2) Wall (3) Generator Outlet (CFD Inlet)
(4) Generator Inlet (CFD Outlet) (5) Package Inlet
(6) Leakage Position 1 & 2 (7) Wall (Temperature Profile)

Figure 5. Boundary setup of the numerical base model [3] modified and used as the design study model (DSM)

To assess kinematic similarity during testing, the flow path of CH_4 leakage (fuel system malfunction) was examined for the real-scale results as well as two operation conditions with $k = 3$ attainable with the actual test rig, namely OP-Ma T232 and OP-Re T232, as seen in figure 6. In the investigated cases the CH_4 jet was ejected (6) into the enclosure in opposing direction to the MEVF (figure 5, LP2). In all cases the MEVF mainly flows over the gear section before evading the inlet casing sideways but proportions of the MEVF also pass the gear side-on or flow downwards after reaching the gear front surface. Afterwards the MEVF enters the gas turbine section by a region of constriction where the flow is partly redirected towards the bottom because of the lesser blockage from the inlet casing. The flow separates at the edge of the inlet casing creating a wake space between the combustion chambers and the inlet casing. During real-scale as well as model-scale operation in Ma-similarity condition, the fuel jet reaches the constriction section around the gas turbine inlet casing before losing momentum and being transported towards the outlets of the enclosure, leaving via both available ducts (1). In both cases the outlet flow features a hemispheric region of outflow near both ducts. In case of Re-similarity operation the fuel

Table 1. Numerical setup of the DSM and TRM

Parameter		Description
Medium		Ideal gas mixture (air and CH_4)
Turbulence model		k-ω SST, automatic wall function
Heat transfer model		Total energy
Advection scheme		High resolution
Simulation type		Steady-state
Boundary	**Type**	**Physical property**
1	Outlet (air & CH_4)	Static pressure
2	Wall	No slip wall Adiabatic
3	Inlet (air)	Velocity Static temperature
4	Outlet (air)	Velocity (DSM) Mass flow (TRM)
5	Inlet (air)	Velocity Static temperature
6	Inlet (CH_4)	Velocity Static temperature
7	Wall	No slip wall Temperature profile

jet is displaced almost immediately after ejection. Since the jet can be assumed to be in choked condition, operating the rig in Re-similarity condition would result in an imbalance of momentum ratio between the fuel jet and the MEVF, thus explaining the deviant behavior illustrated in figure 6*c*. Afterwards the air-fuel mixture is transported into a recirculation zone underneath the gas turbine diffuser before ascending spirally and being carried away by the MEVF, exiting through one outlet duct only. For this configuration the global outlet flow appears to be more directional as it changes towards a jet-type flow compared to the previously regarded cases, leading to lesser kinetic similarity to the real-scale machine as also illustrated in figure 3*a*.

These results indicate that Ma-similarity shall be preferred for kinematic similarity, especially when investigating leakage dilution. For separate investigation of buoyancy effects with correct ratio of thermal lift and inertia, Ar-similarity would also represent a viable setup. Re-similar operation condition however is still necessary when measuring heat transfer, as mentioned in section 2.2, e.g. for applying realistic heat transfer boundary condition in CFD investigations. Therefore, based on the analytical and numerical design studies a model scale of 1:3 was chosen while determining that the ventilation system has to be able to accomplish Ar, Ma- as well as Re-similarity operation condition.

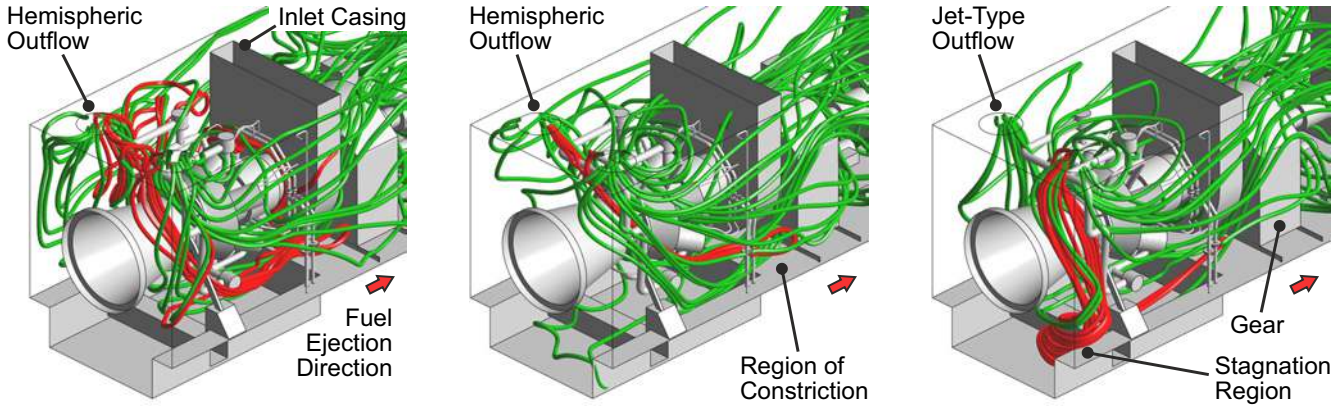

(a) 1:1 **(b)** 1:3 OP-Ma T232 **(c)** 1:3 OP-Re T232

Figure 6. Flow path of the diluted CH_4 leakage jet (red) being released from leakage position 2 (figure 5, LP2) in opposing flow direction to the MEVF (green) near the hot gas turbine components using the DSM

2.4 Test Rig Construction

To achieve Re-similarity during testing a total of four dual-stage counter-rotating fans had to be installed. Like in the actual turbine package these blowers are set up in parallel-path air flow arrangement at the air inlet as well as at the air outlet side (see figure 1). Though all fan stages could have been arranged at the inlet side of the test rig leading to a less complex set up and reducing the construction height, testing of individual fan path failure would have been limited to three out of fifteen possible cases. By utilizing the fan arrangement seen in figure 1, the rig ventilation flow also features the combined suction and pressurized operation condition in an open cycle as applied to the real-scale machine. Since available ventilation systems could not deliver the required performance for Re-similarity at the scaled model's resulting duct diameter, larger dual-stage counter-rotating fans were chosen. The required nozzles and diffusers were designed as a trade-off between construction length and pressure loss obtained by hydraulic correlations [8]. Especially the usage of nozzles and additional piping for instrumentation (see figure 10*a*) at the package inlet can be expected to reduce the wake resulting from the fan motor and hub while the counter-rotating configuration presumably will reduce the inlet swirl. The impact of these deviations will be investigated in detail numerically after the validation procedure.

To avoid transmission of vibrations from the main ventilation fans into the package enclosure the connection pipes at the in- and outlet are decoupled by using flexible hose piping. The test rig additionally features eight small-scale high-performance fans operating at up to 11,000 RPM to include and to control the IGCF within the generator casing (see figure 2). The overall test rig properties and performance data are given in table 2. In order to keep the test rig weight and cost at acceptable levels, most of the gas turbine components were constructed from thin sheet metal with standard parts being used for providing the structural integrity of the package base frame and the fan support. The enclosure housing was built from modular profiles incorporating easily removable window segments for convenient window maintenance and test rig access. Pipework of the fuel and the oil system was constructed from standard tubes. Since the velocity field within the enclosure is of main interest, optical measurements were chosen as the primary measurement technique. Therefore, all side and roof walls except the ones which are flange-mounted to the package fans were constructed from transparent material (see figure 1). Due to the addition of heating elements in the following phase of the project, Perspex was discarded and borosilicate glass was chosen for its higher temperature resistance as well as for its high optical quality.

Table 2. Test rig properties and performance data

Dimensions		Value	Unit
Model scale		1:3	-
Enclosure Volume		3.63	m^3
Performance	**OP-Ma**	**OP-Re**	**Unit**
Flow rate MEVF	5,584	16,707	m^3/h
Flow rate IGCF	3,111	9,308	m^3/h
Room changes	25.6	76.7	$1/min$

High surface temperatures at the gas turbine model components can be obtained by attaching silicone rubber heaters to their inner surfaces without changing the outer geometry. However, the real temperature levels cannot be realized due to the aforementioned safety aspects and limitations of the silicone mats, leading to a wall temperature limit of approximately 220 °C. A numerical model of the gas turbine as a 1-D thermal network was developed as seen in figure 7. All relevant components of the gas turbine were modeled as thermal capacitances (C_i) and were coupled through heat conduction ($G_{\lambda,i}$) to each adjacent component as well as to the MEVF ($\dot{m}$, $\dot{Q}_{conv}$) via convective heat transfer ($G_{h,i}$).

The applied heat transfer coefficients were determined from CFD results using the DSM. The estimated heating powers for the different sections ($\dot{Q}_{el,i}$) indicate that with the given geometry and materials the desired temperature distribution can be obtained well. During heated operation condition the surface temperatures will be controlled by a closed-loop circuit and measured via thermal imaging.

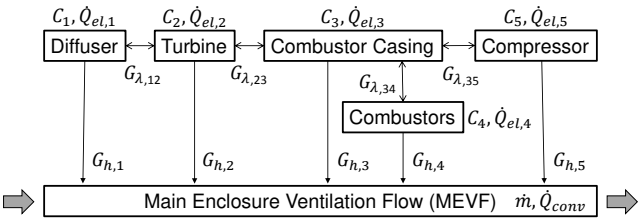

Figure 7. Thermal network model of the gas turbine components for heating element design

To allow leakage investigations for explosion safety assessment in the test rig, the pipework corresponding to the fuel system was designed for pressurized operation with gas supply access below the main frame. Carbon dioxide, selected as the model leakage gas, can exit the fuel piping at specific locations, e.g. flanges or seals. These parts can be made permeable by loosening fixing screws, seal removal, or installing perforated disks in order to simulate worst-case failure scenarios like fuel jet ejection into zones of recirculation. A gas concentration measurement system with sensors at several representative positions inside the enclosure and at the outlet will provide validation data for numerical results of leakage gas distribution and dilution. After validation the CFD model can then be used to investigate leakage cases of real engine fuel and will allow more reliable explosion safety investigations.

3. CFD STUDY OF THE ACTUAL TEST RIG

During the course of the test rig development the design of the actual gas turbine package was optimized further, leading to slight differences in component arrangements. To accomplish maximum accuracy of the project results, a new numerical flow model of the test rig (TRM) was created to be used for validation purposes. This model was generated using ANSYS ICEM and ANSYS CFX 17.0. A grid sensitivity analysis was carried out as well as investigations on the flow field in cold configuration without leakage for a Re-similarity volume flow and adiabatic wall temperatures (OP-Re AWT). Re-similarity was chosen to allow adjustment of y^+ at a velocity level suitable for future heat transfer investigations.

Similar to the work of Petrick [3] the simulations were carried out with a steady-state approach, which is commonly used for investigations of enclosure ventilation [9]. Best practice guidelines on conducting CFD investigations in gas turbine enclosures are available from Ivings *et al.* [9] and in a more general form from Casey *et al.* [10] and were taken into account during the course of model generation. The investigations of Petrick [3] proved the validity of using a combined tetrahedron and prism meshing approach, therefore it was incorporated during the investigations of the TRM. At first the grid study was carried out utilizing only tetrahedron-type elements while varying the element size globally without resolving the boundary layer (no BLR) to ensure sufficient resolution within the core flow region. Subsequently prism-type elements were included in the mesh to separately add boundary layer effects to the core flow phenomena.

Since heat transfer investigations shall be conducted in the future, these mesh configurations resolve the boundary layer (BLR) with y^+ values around 1 on the gas turbine surfaces and y^+ values under 11 for the remaining domain walls to avoid transition through the buffer region of the near wall flow. The boundary layer is resolved with 13 elements perpendicular to the surface wall at an expansion ratio of 1.5, chosen based on a trade-off between element count, cell volume change within the boundary layer as well as between the outer prism element and the adjacent tetrahedron core flow mesh. During the refinement process of the BLR meshes, the total height and therefore spacing of the boundary layer elements was kept constant and only the element count along the bounding walls was varied. The influence of the mesh resolution on the dimensionless pressure loss coefficient ζ is given in figure 8 for a model setup without and with BLR.

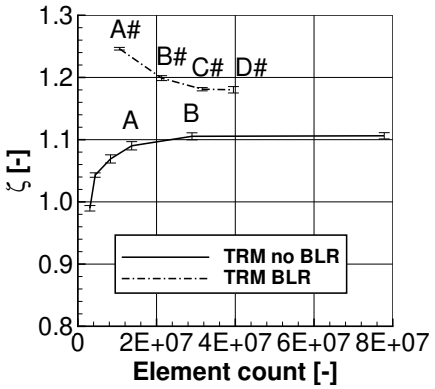

Figure 8. Grid sensitivity study of the TRM

ζ is calculated as defined in equation 7 with Δp_{tot} being the area-averaged total pressure difference between package inlet and outlet ducts and $p_{dyn,in}$ the area-averaged dynamic pressure at the inlet ducts.

$$\zeta = \frac{\Delta p_{tot}}{p_{dyn,in}} \tag{7}$$

Due to the high complexity of the flow problem, most flow quantities do not converge asymptotically towards a constant value over the course of simulation iteration but rather fluctuate around a mean value. When evaluating only the last iteration step of such steady-state simulations, the results can vary depending on the state of the local fluctuations. Therefore, all calculations were carried out over 2000 iteration steps with the results being averaged over the last 1000 steps. The averaged value of ζ is then displayed along with

its corresponding standard deviation during the averaging interval, thus minimizing errors due to fluctuations in the flow field while maintaining information about the degree of fluctuation quantitatively.

With the first investigated mesh without BLR and about 3 million elements, ζ was obtained to be just below unity. During the course of refinement ζ increases and converges to a value of about 1.11 for a cell count of about 29 million elements. Increasing the element numbers by more than a factor of two to a total of about 77.8 million elements leads only to an insignificant change of ζ. Based on the results without BLR mesh A could have been chosen as being sufficiently resolved. To prove this assumption is also valid for models with BLR, additional meshes A# and B# were created incorporating the previously described prism element distribution near bounding walls as well as the same global element size as mesh A and B, respectively. When resolving the boundary layer the overall level of ζ is increased and it decreases over mesh refinement. In contrast to the non-BLR configurations neither A# nor B# can be regarded as sufficiently resolved and therefore further refinement was investigated utilizing meshes C# and D# which resulted in significantly lower values compared to B# but insignificant differences to each other. This indicates that pressure losses are resolved sufficiently in the core flow as well as in the near wall regions leading to mesh C# being chosen as the grid study's resulting mesh with a value of ζ around 1.18 and 31.6 million elements.

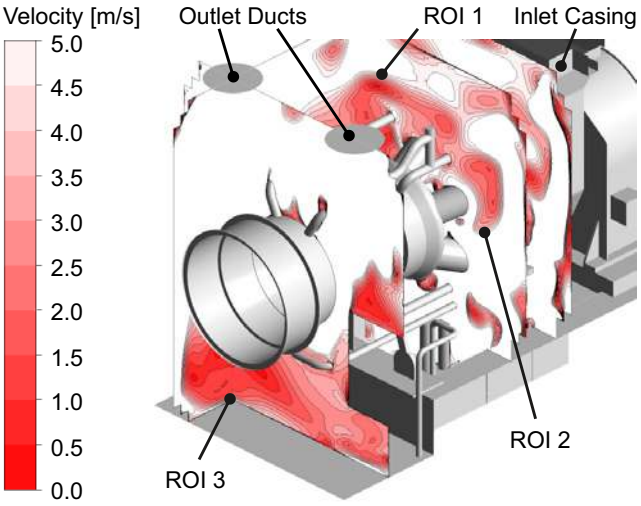

Figure 9. Distribution of stagnation regions within the enclosure near the gas turbine for the TRM using mesh C# in OP-Re AWT

In addition to the velocity profiles near the enclosure inlet and outlet ducts as well as around the generator casing the occurring stagnation regions are of interest for PIV measurements, CFD validation and future leakage dilution investigations. To identify these regions of interest (ROI), which are located especially around the hot gas turbine components, the TRM with the chosen mesh C# was analyzed as illustrated in figure 9. Generally the MEVF is well designed, with only some stagnation regions remaining. Due to the blockage of the inlet casing a wake space occurs between the combustion chambers and the inlet casing (ROI 1 and ROI 2), similar to the flow observed in figure 6*c*. Since the flow is redirected downwards at the inlet casing, only smaller stagnation regions remain underneath the combustion chambers. ROI 3 is located underneath the gas turbine diffuser. Though the ventilation system would have diluted any possible leakage being transported to ROI 3 way below its lower explosion limit, long term accumulation could still lead to explosive air-fuel mixtures. Therefore, ROI 3 should also be considered.

4. TEST RIG INSTRUMENTATION

Having a large test rig with multiple regions of interest, Particle Image Velocimetry (PIV) was selected as the main technique for measuring the flow field inside the enclosure, since it allows the acquisition of complete 2-D (or with Stereo-PIV even 3-D) vector fields over large image planes at one instant. The required double-shutter camera and the laser sheet optics are mounted perpendicular to each other using profile frame constructions adaptable to the model enclosure. Thereby, PIV images can be recorded under various orientations from several positions around the enclosure, since optical access is given by the glass windows with only few shadowed or hidden regions remaining due to geometrical restrictions.

Further standard measuring equipment, consisting of several pressure and temperature probes, mainly serves for monitoring the test rig's operation point at the package inlets, outlets and the generator volume flow rate during PIV imaging in order to create definite, comparable flow behavior under varying environmental conditions (see figure 10). Total pressure probes combined with Type-T thermocouples as well as static wall pressure taps are installed at each inlet and outlet duct for measuring the flow rates and the overall pressure loss of the package (setup 1 figure 10*a*). The angular adjustable probes can be traversed along two perpendicular axes in order to determine the flow velocity profiles and the swirl of the inflow resulting from the main ventilation fans as well as of the outflow for every operation condition. At the generator inlet opening a traversable rake with 10 pitot tubes provides the inflow total pressure and velocity field in combination with wall pressure taps inside the generator casing (setup 2 figure 10*b*). Additional pressure probes or static wall pressure taps can be deployed around the enclosure as required by utilizing the modular test rig design, e.g. replacing the glass plates within the window modules with instrumented metal sheets, thus allowing additional measurements for CFD validation purpose at several regions of interest. Pressure signals are transferred to two pressure transducer arrays (Scanivalve ZOC17IP/8PX) and recorded by a data acquisition system (NI PXI), which are located in a temperature-controlled room.

At the package inlet time-resolved velocity measurements will be carried out within the region of the free jet using 1-D Constant Temperature Anemometry (CTA) probes, as the

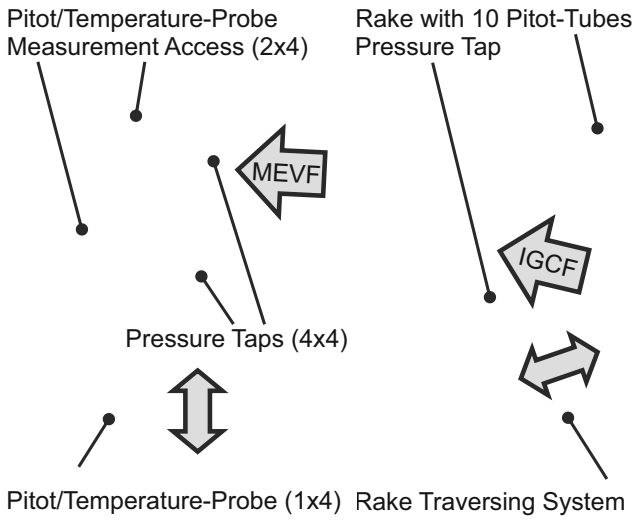

(a) Package in- and outlets (Probe setup 1)

(b) Generator inlet (Probe setup 2)

Figure 10. Test rig instrumentation for operation point monitoring and flow profile measurements

turbulence intensity is one of the main quantities when investigating heat transfer effects experimentally as well as numerically.

5. CONCLUSION AND OUTLOOK

A scaled test rig of a state-of-the-art MGT-6100 gas turbine package from MAN Diesel & Turbo SE was developed with focus on the ventilation flow within the enclosure to be used for experimental and numerical explosion safety investigations. Therefore, the gas turbine components were designed mainly as flow obstacles and do not feature any combustion system or power output. During the course of development, analytical as well as CFD-based studies were carried out to identify a model scale which is both feasible and allows the best possible results in terms of transferability to the real-scale machine, even under operation condition restrictions in the test facility. Due to the complex nature of the flow within the enclosure, several aspects were taken into account like heat transfer, natural convection, the interaction of the MEVF and IGCF as well as the momentum ratio of the MEVF and possible fuel leakage flows for cases of engine failure. These studies showed that a model scale of 1:3 represents the best trade-off between similarity, construction effort, and cost and that the ventilation system has to be able to accomplish Re-similarity operation condition. Allowing all possible cases of fan failure to be investigated experimentally, the test rig features fans at the inlet and outlet ducts of the enclosure, as seen in the real-scale machine. Changes of component arrangement in the actual package led to the creation of an additional CFD model, which was used to obtain regions of interest for PIV measurements.

Future work will include the commissioning of the enclosure test rig as well as PIV measurements in cold configuration. These results will then be used to comprehensively validate the TRM, which shall be used to carry out detailed investigations on the flow structure within the enclosure. The test rig will then be modified to investigate the optimization potential of the MEVF inlet orientation being changed from horizontal to vertical as well as to feature heated gas turbine components and gas supply for leakage investigations. These results can be used to validate the TRM even further and will allow more comprehensive explosion safety investigations in the future.

ACKNOWLEDGMENTS

The development work was conducted as a part of the joint research program COORETEC-Turbo. The work was supported by the Bundesministerium für Wirtschaft und Technologie (BMWi), as per resolution of the German Federal Parliament under grant number 03ET7030B. The authors gratefully acknowledge COORETEC-Turbo and MAN Diesel & Turbo SE for their support and permission to publish this paper. Additionally, this publication was supported by the Ruhr University Research School PLUS, funded by Germany's Excellence Initiative [DFG GSC 98/3]. The responsibility for the content lies solely with its authors.

NOMENCLATURE

Latin Symbols

Ar	[-]	Archimedes number
C	[J/K]	Thermal capacitance
c	[m/s]	Package inlet velocity
D	[m]	Package inlet duct diameter
f	[-]	Ratio of quantities
G	[W/K]	Thermal conductance
Gr	[-]	Grashof number
g	[m/s^2]	Gravitational acceleration
h	[W/m^2K]	Heat transfer coefficient
k	[-]	Model scaling factor
	[W/mK]	Thermal conductivity
L	[m]	Characteristic length
Ma	[-]	Mach number
		Ma-similarity operation condition
$\dot{m}$	[kg/s]	Mass flux
Nu	[-]	Nusselt number
		Nu-similarity operation condition
Pr	[-]	Prandtl number
p	[Pa]	Pressure
$\dot{Q}$	[W]	Heat flux
Re	[-]	Reynolds number
		Re-similarity operation condition
T	[K]	Ambient temperature
y^+	[-]	Dimensionless wall distance

Greek Symbols

β	[1/K]	Coefficient of thermal expansion
Δ	[Var.]	Difference
ν	[m^2/s]	Kinematic viscosity
ϕ	[Var.]	Generic flow variable
	[-]	Generic dimensionless quantity
ζ	[-]	Dimensionless pressure loss coefficient

Subscripts

conv	Convective heat flux
dyn	Dynamic pressure
el	Electric heating power
h	Convective thermal conductance
in	Property at package inlet
M	Property at model scale
O	Property at real scale
tot	Total pressure
λ	Conductive thermal conductance

Abbreviations

AWT	Adiabatic wall temperature
BLR	Boundary layer resolution
CAD	Computer-aided design
CFD	Computational fluid dynamics
DSM	Design study CFD model
IGCF	Internal generator cooling flow
MEVF	Main enclosure ventilation flow
OP	Operation condition package enclosure
PIV	Particle image velocimetry
ROI	Region of interest
SST	Shear stress transport turbulence model
TRM	Test rig CFD model
T232	Wall temperature profile with 232 °C limit
VDI	Verein Deutscher Ingenieure e.V.

REFERENCES

[1] E. Aschenbruck, M. Cagna, V. Langusch, U. Orth, A. Spiegel, A. Wiedermann, and S.-H. Wiers. MAN's new gas turbines for mechanical drive and power generation applications: GT2013-94897. In *Proceedings of the ASME Turbo Expo 2013*, New York, 2013. ASME.

[2] Health and Safety Executive. Fire and explosion hazards in offshore gas turbines: Offshore information sheet no. 10/2008. Aberdeen, 2008.

[3] S. Petrick. Untersuchung der Strömungsverhältnisse innerhalb einer Gasturbinenschallhaube. Master's thesis, Hochschule Bochum, Bochum, 2012.

[4] D. Vahidi, H. Bagheri, and B. Glezer. Numerical and experimental study of ventilation for gas turbine package enclosure: GT2006-90960. In *Proceedings of the ASME Turbo Expo 2006*, New York, 2006. ASME.

[5] M. Ivings, S. Clarke, S. Gant, B. Fletcher, A. Heather, D. Pocock, D. Pritchard, R. Santon, and C. Saunders. Area classification for secondary releases from low pressure natural gas systems: Research Report (RR) 630. Health and Safety Laboratory, Buxton, 2008.

[6] VDI e.V. Engineering methods for the dimensioning of systems for the removal of smoke from buildings: VDI 6019 Beuth, Berlin, Juli 2009.

[7] VDI e.V. VDI Heat Atlas. Springer, Berlin, 11. ed., 2013.

[8] I. Idelčik. Handbook of hydraulic resistance: Coefficient of local resistance and of friction. Israel Program for Scientific Translations, Jerusalem, 1966.

[9] M. Ivings, C. Lea, and H. Ledin. Outstanding safety questions concerning the analysis of ventilation and gas dispersion in gas turbine enclosures: Best Practice Guidelines for CFD. 2003.

[10] M. Casey and T. Wintergerste. Best practice guidelines ERCOFTAC Special Interest Group on Quality and Trust in Industrial CFD: Version 1.0. ERCOFTAC, 2000.